INTERNATIONAL SOCIETY FOR SOIL MECHANICS AND GEOTECHNICAL ENGINEERING

SIMSG   ISSMGE

Scour development around complex offshore foundations under current load

Mario Welzel,[1] Alexander Schendel,[1] Ramish Satari,[2] Arndt Hildebrandt,[1] Insa Neuweiler[2] and Torsten Schlurmann[1]

[1]Ludwig-Franzius-Institute for Hydraulic, Estuarine and Coastal Engineering, Leibniz University of Hanover, [2]Institute of Fluid Mechanics and Environmental Physics in Civil Engineering, Leibniz University of Hanover, email: schendel@lufi.uni-hannover.de, satari@hydromech.uni-hannover.de, hildebrandt@lufi.uni-hannover.de, neuweiler@hydromech.uni-hannover.de, schlurmann@lufi.uni-hannover.de

*Corresponding author: welzel@lufi.uni-hannover.de

ABSTRACT

The expansion of offshore wind energy motivates the development of unique foundation structures, resulting in unique prototypes such as the structure introduced in this study. However, distinct knowledge gaps still exist regarding the description and prediction of scour around complex foundation structures. In this context, this study aims to contribute to the understanding of scour around offshore wind foundations by experimentally evaluating and comparing the sensitivity of spatio-temporal scour for live-bed conditions between the introduced gravity-based structure and a conventional four leg jacket structure. Furthermore, the deposition pattern behind the gravity-based structure is investigated and contrasted against current knowledge of more simple jackets. The tests focused on steady flow (current-only), live-bed conditions. The bed topography is measured for 15-, 90- and 420-minutes testing time with a 3D laser scanner. A dimensionless correlation reveals a spatial erosion intensity 2.5 times larger for the gravity-based structure compared to the conventional one.

INTRODUCTION

As an important part of the renewable energy sector, the growth of offshore wind capacity has accelerated significantly in recent decades (WindEurope, 2021). However, the current growth is not sufficient to meet the renewable energy targets set by the European Union to achieve its goal of climate neutrality by 2050 (EU, 2020). Sites suitable for offshore wind energy expansion are highly contested and have to be shared with other stakeholders. In order to increase energy output and improve efficiency, sites are increasingly being developed further from the coast and in greater water depths (WindEurope, 2021). As a consequence, complex foundation structures such as jackets are becoming more common. These structures provide a higher level of structural stability, which is also essential for future offshore mega-structures with a hub height of more than 200 m. As discussed in Welzel (2021), the interaction of large and complex foundation structures with the surrounding flow and seabed is not yet fully understood. While the equilibrium scour depth around monopile foundations has been studied quite extensively in the past (e.g. Melville and Coleman, 2000; Sumer and Fredsøe, 2001; 2002; Schendel et al., 2020), there are only a few systematic studies (Chen et al., 2014; Baelus et al., 2019; Welzel et al., 2019a; Welzel et al., 2020) investigating the phenomena of scour development around complex substructures. The term

complex refers in the following to the structural geometry and relates it to a simple monopile, e.g. the introduced structure and conventional jackets are referred as complex.

The development of scour at complex offshore structures differs from that at monopile structures in that global erosion occurs in addition to local scour. Large spatial morphological changes and displacement of large amounts of sediment may occur, with potential detrimental consequences for marine ecosystems or degradation of the structural stability. While topics dealing with the pointwise scour development are more frequently investigated, spatial patterns regarding erosion or deposition have been far less investigated as they are not in focus when assessing structural deterioration, but are a key aspect when dealing the morphological footprint of marine infrastructure in reference to potentially harmful effects in the marine environment. Considering the general trend of the installation of more complex foundation structures as jackets, this is an important knowledge gap concerning the safety of such installations as well as their overall impact on the marine environment.

The investigated structure represents a combination of a six-legged jacket structure and a gravity foundation with suction buckets. An idea of the structure was to handle a structure light as a jacket during the installation and ballast the 6 containers afterwards to benefit of a gravity-based structure. Whilst there is no experience with these structures in regard of its environmental impact, it is expected that this unconventional structure will interact with a flow in a unique way and that the scour process will be significantly different to more conventional jacket structures. By comparing different structures, an unconventional, hydrodynamic compact structure with a more hydrodynamic transparent common jacket structure, we aim to get a better understanding of scour around complex offshore wind foundation structures and to allow an assessment of the structure-induced morphological footprint (Welzel, 2021). The main objectives are:

- To perform high resolution measurement of the spatio-temporal evolution of the scour process with 3D-Scans at different time periods under current load.
- To analyze the scouring process around a unique jacket-type structure in live-bed conditions.
- To determine and evaluate spatio-temporal scour patterns as a balance of eroded and accumulated sediment volumes.
- To correlate the spatio-temporal scour patterns with the erosion around a conventional jacket structure.

With these measurements and the analysis it will be possible to identify processes relevant to the scour development around unconventional structures that would be missed in planning processes and to identify the conditions when such processes occur.

EXPERIMENTAL SETUP & PROCEDURE

In order to allow a reasonable comparison between the two structures, the unconventional gravity-based jacket structure and a more common 4-legged jacket structure, the procedure and general setup are consistent with those of Welzel et al. (2019b, 2020). As large parts of the experimental setup are identical, this chapter describes only the essential parts of the experimental setup. More detailed information about the facility and the common 4-legged jacket structure can be found in Welzel et al. (2019b, 2020). Physical model tests at a scale of 1:45 were performed in the 3D wave-

current basin of the Ludwig-Franzius-Institute, Leibniz University Hannover, Germany. The 3D wave basin has a total length of 40 m and a width of 24 m, with a maximum possible water depth of about 1 m (see Figure 1). A unidirectional current is superposed that propagates from left to right, see Figure 1. The current is generated by a pump system consisting of four pumps with a total combined maximum discharge of 5 m³/s.

The unique gravity-based jacket foundation (original design concept from the Maritime Offshore Group) consists of an upper 6-legged jacket structure with a large container at each leg. The purpose of these containers is to provide buoyancy during transport of the jacket to the installation site. Once on site, these containers can be continuously filled with sand or stones to allow the jacket structure to slowly sink to the seabed. However, the containers do not sit on the seabed. Instead, each container rests at a certain distance from the seabed to reduce the flow obstruction. Finally, the jacket is secured to the seabed by suction buckets. The model of the gravity-based jacket foundation structure was 3D-printed in polyamide plastic. Subsequently, the individual printed parts have been attached and glued to each other building a rigid body. The six suction buckets were made out of steel with an extra deep embedment into the sediment and a stiff connection to the flume bottom to investigate the erosion potential. At the beginning of the test, the top of the suction buckets was 3 cm above the sediment bed. Dimensions of the unique gravity-based and conventional 4-legged jacket structure are given in Figure 2.

Sand with a median grain diameter of $d_{50} = 0.19$ mm, a density of $\rho_S = 2.65$ g/cm³ and a geometric standard deviation of $\sigma_S = \sqrt{d_{84}/d_{16}} = 1.4$ was used for the experiments. A photograph of the experimental setup is shown in Figure 1. The scour and erosion pattern were measured by using a high-resolution 3D laser scanner (Faro Focus). Ensuring a good compaction, the sand was installed in wet conditions and loaded during several pre-tests to ensure no settlement of the sediment during the tests. Three tests have been conducted under current only conditions with a depth averaged velocity of 0.417 m/s, representing live bed conditions. The spatial scour pattern was measured after 15 min, 90 min and 420 min loading time. For the scour measurements, the wave basin had to be carefully drained to avoid any influences of the water on the scour pattern. Subsequently, the bed topography was measured with the 3D laser scanner. While being time-consuming, this measurement procedure allowed a detailed look into the temporal evolution of spatial scour patterns. The test conditions are summarized in Table 1. Current induced flow velocities were
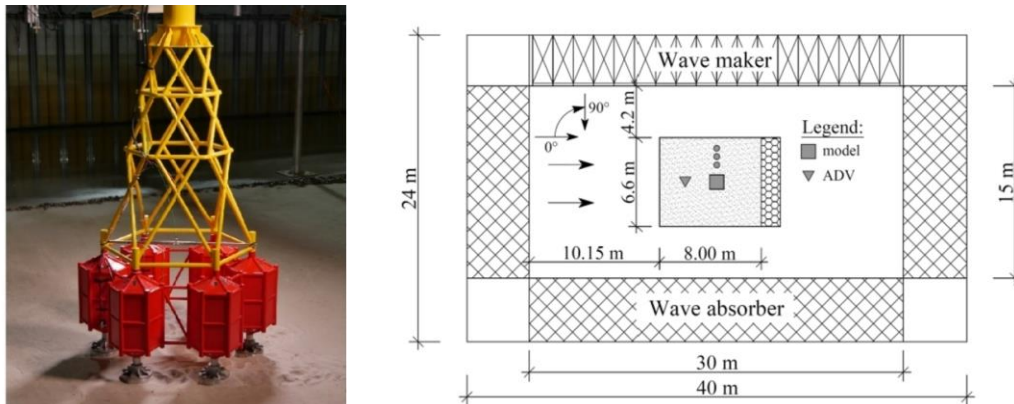

Figure 1. (left) Photo of the jacket gravity foundation structure used in test 1a – 1c (right) experimental setup in the wave-current basin, plan view, current coming from left to right.

measured by means of an Acoustic Doppler Velocimeter (ADV) (Vectrino+, Nortek AS, Norway), positioned 2.5 m upstream of the model (in current direction), see Fig. 1. The ADV has been installed at a distance of 10 cm (2.5D) above the sediment bed. In the following, the current velocity at this position is referred to as U_c. Additionally, a vertical profile of the streamwise flow velocity was collected to determine the undisturbed, depth averaged current velocity $\overline{U}$.
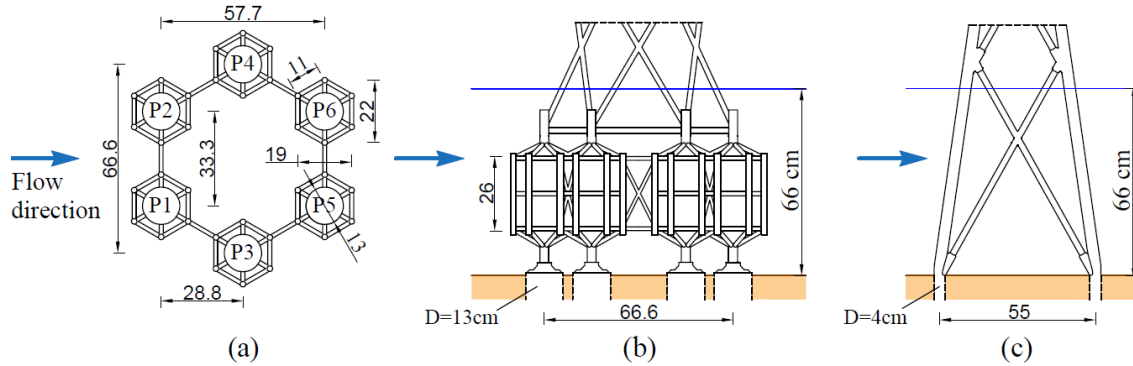

Figure 2. Schematic view on the models: (a) plan view gravity-based jacket (b) side view gravity-base jacket (c) side view 4-legged jacket, including dimensions and water depth

Table 1 - Test conditions and parameters, for Test 1a-1c D for jacket = pile, Test 2a-2c, D gravity-based structure = suction buckets, structure footprint see also Figure 2

Test	Current velocity 10 cm above bed U_C	Depth averaged velocity $\overline{U}$	Shields Parameter θ	Test duration	Structural reference diameter D	Structure footprint size
	[m/s]	[m/s]	[-]	[min]	[cm]	[cm]
1a	0.388	0.417	0.084	15	13	67 x 58
1b	0.388	0.417	0.084	90	13	67 x 58
1c	0.388	0.417	0.084	420	13	67 x 58
2a	0.388	0.417	0.084	15	4	55 x 55
2b	0.388	0.417	0.084	90	4	55 x 55
2c	0.388	0.417	0.084	420	4	55 x 55

Calculation of spatial erosion parameters

In the present study we use an approach to analyze displaced sediment volumes previously introduced in Welzel et al. (2019b, 2020) to investigate and compare complex erosion and deposition patterns around offshore wind foundation structures. The approach is only briefly explained here. For a more detailed explanation it is referred to Welzel et al. (2019b, 2020). A displaced sediment volume $\left(V_i = \sum Z_i(a_i) \cdot A_g\right)$ refers to the change of sediment volume related to a specific area a_i. The erosion (topography below the reference pre-scan) or deposition (above pre-scan) volume is simply calculated as the sum of elevation differences Z_i over an area a_i for each grid point within the data matrix, which is then multiplied by the area covered by one datapoint, Ag, which depends on the measurement resolution and grid size. The parameter V_i denotes the "displaced net volume". The "incremental volume depth" $D_{I,i}$ is used as the main parameter to calculate a dimensionless erosion or deposition depth. The value $D_{I,i}$ is obtained by normalizing V_i with the corresponding interrogation area a_i and with a structural reference length

D from a structural element directly obstructing the flow and the soil. In this study the suction bucket diameter of the main piles is used as reference length D to normalize $D_{I,i}$.

$$D_{I,i} = \left(\frac{V_i - V_{i-1}}{a_i - a_{i-1}}\right)/D \tag{1}$$

The lower index refers to the location. The parameter $D_{I,i}$ represents a relative volume change per surface area of a volume $V_i - V_{i-1}$ within adjacent areas $a_i - a_{i-1}$. Increasing rectangular interrogation areas a_i are used to analyze the displaced sediment volumes. This dimensionless representation enables the direct comparison with S/D values, the quantification of erosion volumes as well as the application to predict complex erosion patterns. Similar as in Welzel et al. (2019b, 2020), distances in reference to $D_{I,i}$ are given in this study normalized as multiples of a dimensionless parameter "A", which relates the distances along x and y to the edge length of the structure's footprint. E.g. A = x, y distance/structure footprint distance; e.g., 0.5A = 0.275 m / ((0.67 m+0.58 m)/2) for test 1a – 1c.

RESULTS

Figure 3 shows the scour patterns, each processed by subtracting a post-scan from the related pre-scan of the measured bed topography of tests 1a – 1c. The 3D scans are plotted with an adapted true color colormap in 2.5 cm steps highlighting topographic differences. Additionally, an artificial light source is used for a more natural visualization of the scour pattern. The topography after 15 min loading time (see Table 1, test 1a) is illustrated in Figure 3a and shows the developing scour holes around the structure in an early stage. The size and arrangement of the containers have a large blocking effect on the flow. The approaching flow is deflected to the side or forced under or over the containers. In the cross-section transverse to the direction of flow (see Figure 2), there is only a small unrestricted passage for the flow between pile 1 and 2. As a consequence, flow acceleration might be expected along the centerline. The flow around the suction buckets (diameter=13cm) leads to local scour holes around each suction bucket of the foundation. Pile 1 and 2 lead to an individual scour hole extent of about 3.3 times the diameter of a suction bucket. The center piles P3 and P4 show a slightly smaller scour hole extent of 3D, while the spatial scour extent at the rear piles is reduced to 2.9D for P5 and 2.2D for P6. Interestingly, the topography shown in Figure 3a does not show any significant development of global scour beneath the jacket structure, although the flow obstruction from the containers would suggest flow acceleration beneath the structure. This is highlighted as the topography in the center has only a limited erosion of about 0.15D (2cm) after 15 minutes. The maximum scour depth is observed to be in the range of 0.7D for P1,P2, P5 and P6 and slightly increased on 0.77D for the center piles P3 and P4. The maximum scour depths are located on the inner (direction center of the structure) upstream side, which is consistent with the expectations regarding flow acceleration. The eroded sediment is mainly deposed directly on the rear side of the structure in a distance of 4.3D from the center of the foundation structure with a maximum vertical deposition of about 0.5D. In addition, the formation of ripples downstream of the structure, or rather the absence of ripples,
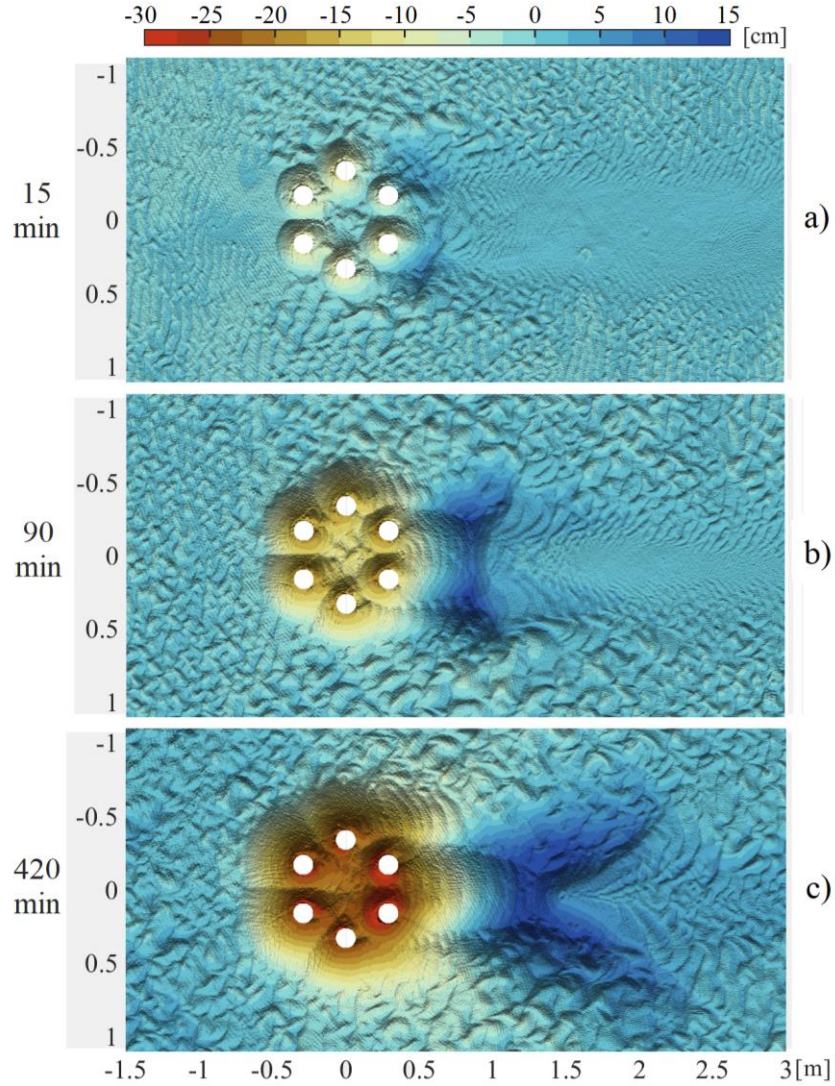
Figure 3. Scour pattern (a) after test 1a and 15 min loading time, (b) after test 1b with 90 min loading time and (c) test 1c for 420 min loading time under live-bed conditions. Colormap in 0.025 cm steps. Current from left to right.

could also be indicative of the overall blocking effect of the structure and, in later stages, that of the sediment deposition. Figure 3b shows the topography after a loading time of 90 minutes. The observed scour pattern is still in an earlier stage. The individual local scour holes are now merged into one large connecting scour hole, similar to that of a scour hole around a pile group. The erosion in the center of the structure still does not reach the depth of scour directly at the suction buckets. The erosion in the center is affected due to the interaction process of the individual local scour holes combined with the general blockage of the structure. However, it is difficult to quantify which process contributes more to the erosion in the center of the structure. The scour extent is increased by about 40-50% in comparison to the topography observed for 15 minutes loading time (Figure 3a). A global scour with a diameter of about 1.2m (9.2D) is formed around the foundation structure. The maximum scour depths can be observed around the individual piles and are of a

similar depth (1.4D-1.5D) for P1-P6. The mean scour depth in the center is also significantly increased on a depth of about 0.9D. The maximum deposition peak are shifted in downstream direction 6.4D from the center of the structure with a maximum vertical offset of 1D. Figure 3c depicts the erosion process after a loading time of 420 minutes. The scour extent is increased by additional 17% (diameter of 1.4m / 10.8D) in reference to test 1b after 90 min. Figure 3c reveals a maximum scour depth of about 2D for the upstream and center piles P1-P4, a scour depth of about 1.7D in the center of the structure as well as scour depths of 2.3D on the downstream side (P5 and P6). As the scour hole is evolved, the fluid-structure-soil interaction has changed. The scoured suction buckets now provide an additional obstacle to the flow, further accelerating the flow in between them and along the centreline. The deposition peak shifted again in downstream direction, with the peak located 9.8D from the center and a maximum vertical deposition offset of 1.3D.
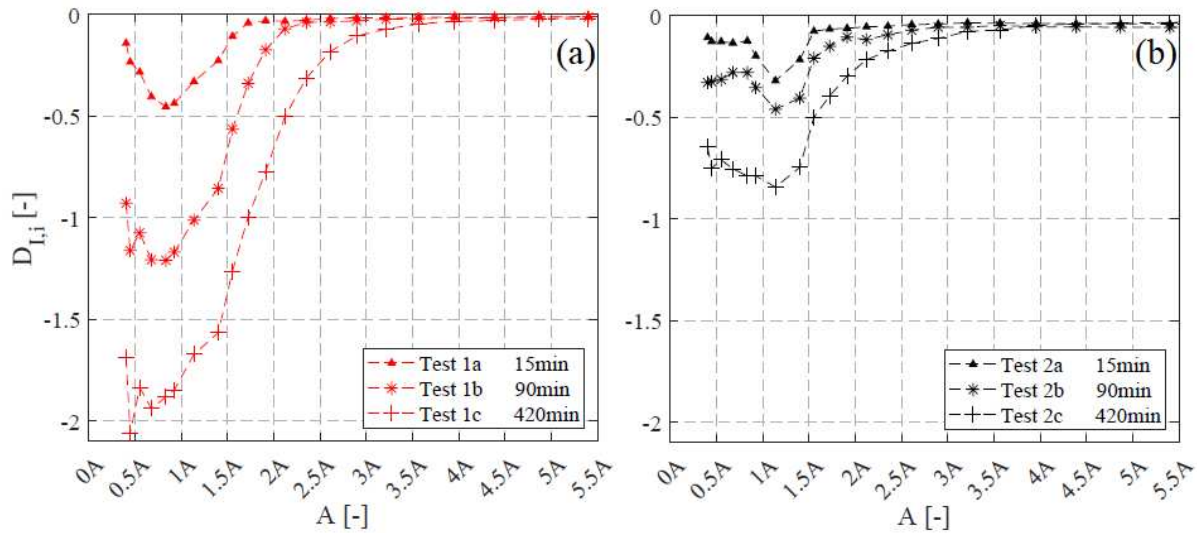

Figure 4. The incremental volume depth $D_{I,i}$ of eroded sediment as a function of the structure footprint "A" (a) depicted for Tests 1a – 1c (gravity-base jacket) and (b) for Tests 2a – 2c (4-legged jacket).

Figures 4a and 4b illustrate the spatial erosion in the vicinity of the foundation structures. Figure 4a shows the erosion for the gravity-based jacket structure, whereas Figure 4b depicts the spatial erosion around the 4-legged jacket structure (same model from Welzel et al., 2019b, 2020). The incremental erosion depths $D_{I,i}$ is calculated for areas between 0.5 (0.5A) and 5.5 times the footprint of the structure (5.5A). For the gravity-based jacket structure, a peak of maximum erosion intensity at 0.7-0.8A emerged after 15 and 90 minutes, which corresponds with the inner part of the scour hole around the main piles. Disregarding the outlier depicted at 0.45A of test 1c, areas smaller than ~0.75A show a declining trend for test 1a-1c with smaller scour depths measured in the center of the structure. A increased erosion intensity is observed in comparison to test 1a in the center at a later stage after 90 and 420 minutes loading time for test 1b and 1c. The observed increased scour depth in the center of the topography seems to be a result of a superposition of the individual scour holes and the global erosion. Areas larger than ~ 0.75A decline in a similar trend for topographies of test 1a-1c, which seems to be dependent of the scour hole erosion angle in the

observed topographies. Figure 4b illustrates the spatial erosion as a comparison around a conventional 4-legged jacket structure. The spatial erosion of test 2a – 2c reveals a peak of maximum erosion intensity at 1.2A, which corresponds with the edges of the scour around the 4 main piles of the jacket. Test 2a shows a maximum value of about $0.3D_{I,i}$, while test 1a reveals a maximum erosion depth of about $0.5D_{I,i}$. Over time, from 15 to 420 minutes, the difference in erosion volumes between the peak at 1.2A and the center of the jacket structure at 0.5A declines, indicating an increasing importance of global erosion processes. The magnitudes of erosion differ significantly between the structures, as test 2c goes up to a maximum of about $0.8D_{I,i}$, while the spatial erosion around the gravity-base jacket (shown in Figure4a) reveals a maximum of about $2D_{I,i}$. Furthermore, a spatio-temporal comparison reveals that the spatial erosion around the gravity-base jacket (Figure 4a) developed faster as the scour around the 4-legged jacket (Figure 4b). This is evident with a comparison of test 1b and 2b. Test 1b, measured after 90 minutes, shows an erosion depth of about $1.2D_{I,i}$ which is about 60% of the final value measured after 420 minutes. In comparison test 2b reveals an erosion depth of about $0.45D_{I,i}$ after 90 minutes, which is about 53% of the final measurement after 420 minutes.
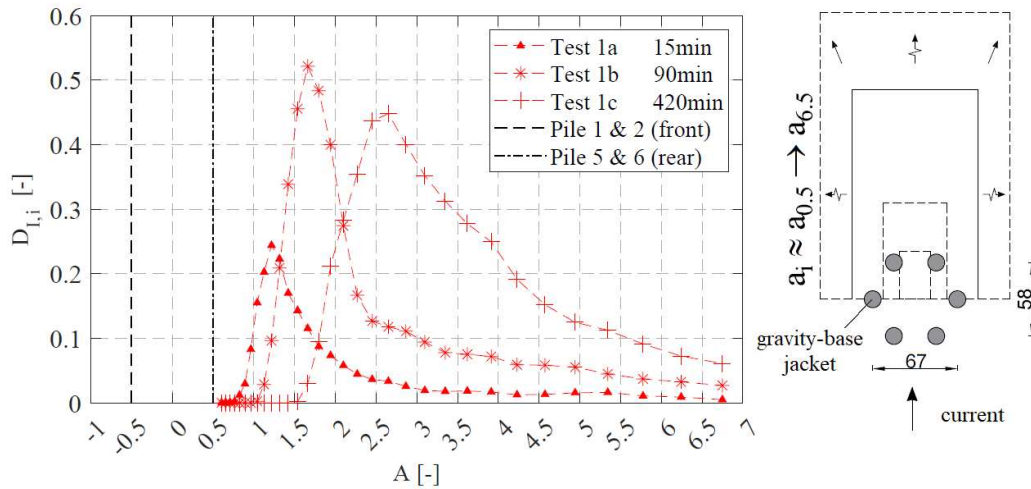

Figure 5. The incremental volume depth $D_{I,i}$ of net deposition as a spatial function of the distance to the center of the gravity-base jacket structure. Additional graphical subset of the arrangement of interrogation areas on the rear side.

Figure 5 illustrates deposited sediment on the rear side of the gravity-base jacket structure. For the calculation of the spatial erosion, as discussed in Figure 4, increasing quadratic areas a_i have been used. To enable the detection of deposited sediment in the far field of the foundation structure, a rectangular type of interrogation area is used to calculate deposited sediment as $D_{I,i}$ (Length= 1.5 times width). For test 1a measured after 15 minutes, the majority of deposed sediment volume is distributed over a distance 1.1 times the structure footprint distance. With longer loading time, an increasing deposition volume together with a shift of the deposition peak is observed. After 90 minutes loading time (test 1b) the majority of the deposed sediment has accumulated at a distance of 1.7 times the structure's footprint and after 420 minutes the peak moved further downstream to

a distance of 2.7 times the structure footprint. Furthermore, the analyses of $D_{I,i}$ also reveals that a considerable increase of deposed sediment ($0.1D_{I,i}$) can be observed even in a distance of up to 5.5 times the structure footprint length.

CONCLUSION

Hydraulic model tests were conducted in the 3D wave and current basin of the Ludwig-Franzius-Institute, to investigate spatio-temporal scour patterns around a unique gravity-based jacket-type structure. This structure significantly obstructs the flow and therefore might be considered as hydrodynamic compact. In order to gain a better understanding of scour around complex offshore wind foundation structures in general, the scour development was compared with that of a conventional four-legged jacket, which can be considered hydrodynamically transparent, in contrast to the gravity-based structure presented. The main conclusions can be summarized as follows:

- The dimensionless approach by Welzel et al. (2019b, 2020) to analyze displaced sediment volumes was applied to correlate the spatio-temporal scour patterns with the erosion around a conventional 4-legged jacket structure. It has been shown that this approach is suitable for the quantification, description and comparison of scour patterns around structures of varying complexity and scale.
- This dimensionless correlation revealed a spatial erosion intensity, measured after 420 minutes, that was 2.5 times larger for the gravity-based structure (max $2D_{I,i}$,) than for the conventional jacket (max $0.8D_{I,i}$,). This result highlights a disproportionate increase in erosion as the complexity and size of an offshore foundation structure increases and thus indicates a potentially large impact of complex structures on the marine environment due to spatial disturbance of the marine seabed.
- The analyses of deposited sediment on the rear side of the gravity-based structure revealed a significant increase ($0.1D_{I,i}$) of deposited sediment even in a distance of up to 5.5 times the structure footprint length from the center of the structure, further highlighting the large-scale morphological changes that can be induced by these structures.

With knowledge of the respective interrogation area size, the "incremental volume depth" $D_{I,i}$ can be directly compared with S/D values or converted into eroded or deposited sediment volumes. But it can also be easily compared with different scales as field data (see Welzel et al., 2019b) or other structure types as shown in the present study.

ACKNOWLEDGEMENTS

REFERENCES

Baelus, L.; Bolle, A.; Szengel, V. (2019). "Long term scour monitoring around offshore jacket foundations on a sandy seabed." In: Proc. of Ninth International Conference on Scour and Erosion (ICSE), Taipei, Taiwan, November 5.-8., 2018.

Chen, H.-H.; Yang, R.-Y.; Hwung, H.-H. (2014). "Study of hard and soft countermeasures for protection of the jacket-type offshore wind turbine foundation." In: Journal of Marine Science and Engineering 2.3, pp. 551-567. DOI: 0.3390/jmse2030551.

EU (2020). EU Strategy to harness the potential of offshore renewable energy for a climate neutral future. European Commission: Brussels, Belgium.

Melville, B.W. and Coleman, S.E. (2000). Bridge Scour. Water Resources Publication, CO.

Schendel, A.; Welzel, M.; Schlurmann, T.; Hsu, T.-W. (2020). "Scour around a monopile induced by directionally spread irregular waves in combination with oblique currents". In: Coastal Engineering 161, 103751. DOI: 10.1016/j.coastaleng.2020.103751.

Sumer, B.M. and Fredsøe, J. (2001). "Scour around pile in combined waves and current." In: Journal of Hydraulic Engineering 127.5, pp. 403–411. DOI: 10.1061/(ASCE)0733-9429(2001)127:5(403).

Sumer, B.M. and Fredsøe, J. (2002). "The Mechanics of Scour in the Marine Environment." World Scientific.

Welzel, M. (2021). Wave-current-induced scouring processes around complex offshore structures. Ph.D. thesis, Gottfried Wilhelm Leibniz Universität: Hannover, Germany. DOI: https://doi.org/10.15488/11225

Welzel, M.; Schendel, A.; Hildebrandt, A.; Schlurmann, T. (2019a). "Scour development around a jacket structure in combined waves and current conditions compared to monopile foundations." In: Coastal Engineering 152, 103515. DOI: 10.1016/j.coastaleng.2019.103515.

Welzel, M.; Schendel, A.; Schlurmann, T.; Hildebrandt, A. (2019b). "Volume-based Assessment of Erosion Patterns around a Hydrodynamic Transparent Offshore Structure." In: Energies 12.16, 3089. DOI: 10.3390/en12163089.

Welzel, M.; Schendel, A.; Goseberg., N.; Hildebrandt, A.; Schlurmann, T. (2020). "Influence of Structural Elements on the Spatial Sediment Displacement around a Jacket-Type Offshore Foundation." In: Water 12.16, 1651. DOI: 10.3390/w12061651.

WindEurope (2021). "Offshore Wind in Europe: Key trends and statistics 2020." Tech. Rep. WindEurope 2021.